

Monitoring the Dynamics of Ligand–Receptor Complexes on Model Membranes

Suman Lata, Martynas Gavutis, and Jacob Piehler*

Institute of Biochemistry, Goethe University Frankfurt/Main, Marie-Curie-Strasse 9, 60439 Frankfurt/Main, Germany

Received July 14, 2005; E-mail: j.piehler@em.uni-frankfurt.de

Ligand-induced receptor oligomerization has been shown to be a general principle for signal propagation across the plasma membrane common to many cell surface receptors.¹ Reduction in dimensionality upon ligand binding onto the membrane has been proposed to have important physicochemical consequences on receptor recruitment and signaling efficiency.^{2–4} Therefore, elucidation of the biophysical mechanisms governing the dynamics of ligand–receptor complexes on membranes is a prerequisite for understanding and for systematic manipulation of signal activation. Owing to a lack of suitable experimental tools, however, the two-dimensional interaction kinetics of ligand–receptor complexes with appropriately mimicked biophysical constraints, including membrane anchoring and membrane fluidity, has hardly been studied quantitatively. Here, we describe an *in vitro* approach for determining a two-dimensional dissociation rate constant of a cytokine–receptor complex.

Chelator lipids incorporated into lipid bilayers have been shown to be powerful tools for tethering histidine-tagged proteins onto solid-supported membranes in an oriented and reversible fashion.⁵ A drawback of the traditional chelator lipids based on a single nitrilotriacetic acid (NTA) moiety, however, is its low intrinsic affinity toward the oligohistidine tag, leading to transient and ill-defined attachment.^{6,7} Measurement of two-dimensional interaction kinetics between membrane-anchored proteins requires stable tethering of a receptor ectodomain by a single histidine tag, and therefore, tethering through traditional chelator lipids is not appropriate.

Recently, we have reported molecularly stable tethering by multivalent chelator headgroups.⁸ Here, we have synthesized a lipid analogue based on a chelator headgroup comprising two NTA moieties (bis-NTA), which binds histidine-tagged proteins with multivalent interactions (Figure 1a). High mobility in the membrane was ensured by conjugating bis-NTA to a saturated and an unsaturated alkyl chain (octadec-9-enyloctadecylamine). This bis-NTA lipid was incorporated into silica-supported, fluid lipid bilayers (Figure 1b). Thus, interactions at the bilayer surface can be studied by surface-sensitive detection while maintaining lateral mobility of proteins attached to the bis-NTA headgroup. This experimental approach was employed to explore the dynamics of ligand-induced ternary complex formation of the type I interferon (IFN) receptor. The extracellular domains of the receptor subunits ifnar1 and ifnar2 fused to a C-terminal decahistidine tag (ifnar1-H10 and ifnar2-H10, respectively) were tethered onto solid-supported membranes (Figure 1b), and complex formation upon binding of the ligand IFN α 2 was monitored in real time by fluorescence and mass-sensitive detection. The dynamics of the ternary complex in plane of the membrane was probed by a displacement assay based on fluorescence resonance energy transfer (FRET) between IFN α 2 and ifnar2-H10 (Figure 1c,d).

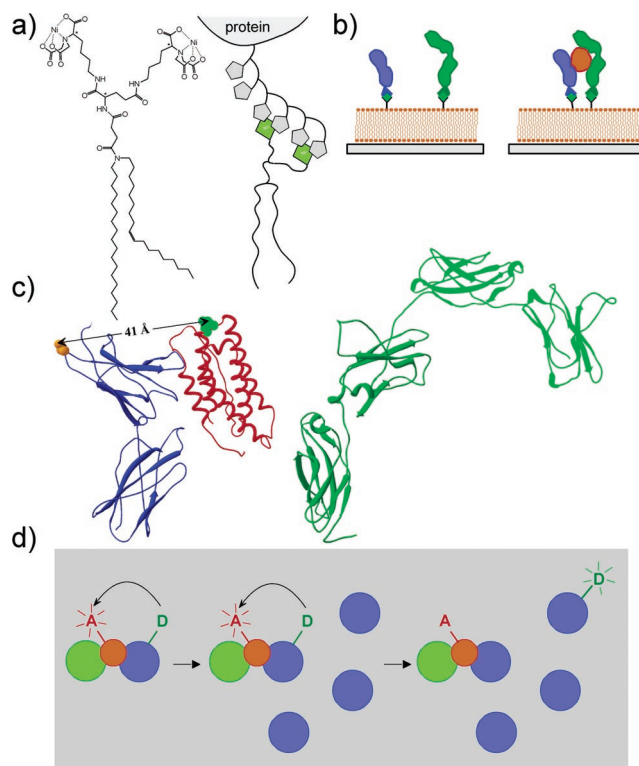


Figure 1. The chemical structure and schematic representation of bis-NTA lipid (a), which binds histidine-tagged proteins by multivalent interaction. (b) Silica-supported lipid bilayers doped with bis-NTA lipid were used for stable tethering of ifnar2-H10 (blue) and ifnar1-H10 (green), and ternary complex formation was induced by binding of IFN α 2 (orange). (c) Structure of ifnar2-EC (blue) in complex with IFN α 2 (red) and a model of ifnar1-EC (green). The residues mutated for labeling are colored in orange (ifnar2-EC) and green (IFN α 2). (d) Principle of surface kinetics measurements by FRET (top view onto the membrane): donor fluorescence from ifnar2-H10 (blue) is quenched upon ternary complex formation with acceptor-labeled IFN α 2 (orange) and unlabeled ifnar1-H10 (green). Upon rapidly tethering an excess of unlabeled ifnar2-H10 onto the membrane, donor-labeled ifnar2-H10 is competed out of the complex, leading to a recovery of the donor fluorescence.

The interaction of IFN α 2 with the two receptor subunits has been studied in detail earlier, and a two-step assembling mechanism was established.⁹

Here, ligand interaction with ifnar2-H10 was monitored by FRET using simultaneous total-internal reflection fluorescence spectroscopy and reflectance interference (TIRFS-RIf) detection.¹⁰ The interaction of IFN α 2 S136C site-specifically labeled with Cy3 (Cy³IFN α 2) with membrane-tethered ifnar2-H10 S35C site-specifically labeled with Alexa Fluor 488 (^{AF488}ifnar2-H10) is shown in Figure 2a. Ligand binding was detected by a drop in the donor fluorescence signal due to FRET from ^{AF488}ifnar2-H10 to bound

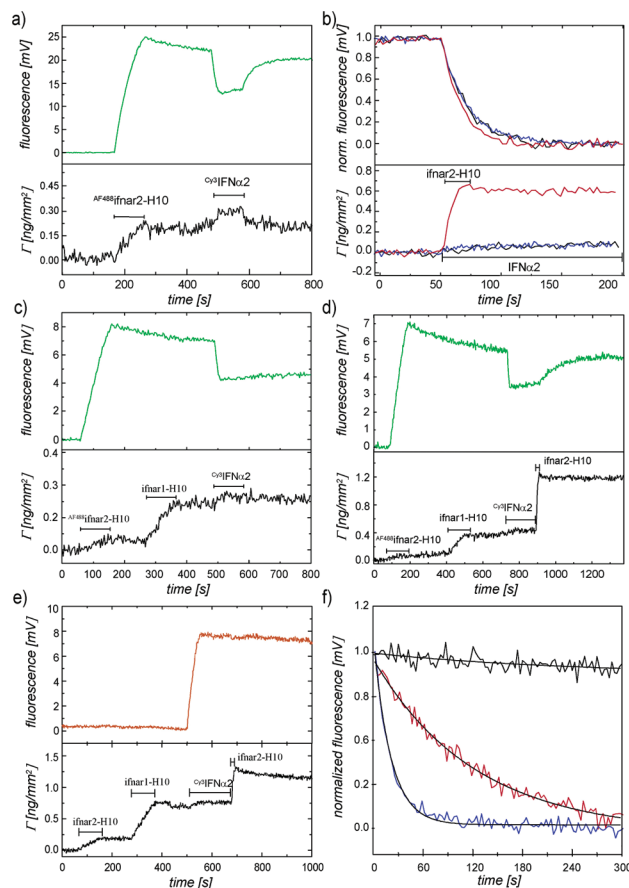


Figure 2. Surface kinetics measurements by FRET. (a) Donor fluorescence detected by TIRFS (upper panel) and mass signal detected by RIF (lower panel) for tethering of AF_{488} ifnar2-H10 (60 nM) onto lipid bilayer followed by binding of Cy_3 IFN α 2 (100 nM). (b) Dissociation of Cy_3 IFN α 2 from AF_{488} ifnar2-H10 upon chasing with IFN α 2 (black) and upon tethering an additional ifnar2-H10 (red) as monitored by FRET (top panel, inverted and normalized fluorescence curves; bottom curves, mass deposition as detected by RIF). For comparison, the dissociation of Cy_3 IFN α 2 from ifnar2-H10 upon chasing with unlabeled IFN α 2 as detected by direct excitation of Cy3 is shown (blue). (c) Interaction of Cy_3 IFN α 2 with AF_{488} ifnar2-H10 and ifnar1-H10 tethered in stoichiometric amounts onto the lipid bilayer as detected by donor quenching. (d) Binding of Cy_3 IFN α 2 (100 nM) to AF_{488} ifnar2-H10 and ifnar1-H10 tethered in stoichiometric amounts onto the lipid bilayer followed by fast tethering of unlabeled ifnar2-H10. (e) Binding of Cy_3 IFN α 2 (detected by direct excitation of Cy3) to unlabeled ifnar2-H10 and ifnar1-H10 tethered in stoichiometric amounts followed by tethering of additional ifnar2-H10. (f) Comparison of the exchange kinetics as detected by the pulse-chase experiment shown in (d) (red) with the dissociation of Cy_3 IFN α 2 from AF_{488} ifnar2-H10 alone as shown in (b) (blue) and the dissociation of Cy_3 IFN α 2 from the ternary complex as shown in (e) (black).

Cy_3 IFN α 2. During ligand dissociation, the fluorescence signal recovered, confirming ligand-specific fluorescence quenching. As the interaction between IFN α 2 and ifnar2-H10 at surfaces was shown to be strongly biased by mass transport limitation,¹⁰ ligand dissociation unbiased by rebinding was measured by chasing the receptor–ligand complex with 1 μ M nonlabeled IFN α 2 in solution, and by tethering an excess of nonlabeled ifnar2-H10 to the surface (Figure 2b). Similar dissociation kinetics with a k_d of 0.05 ± 0.005 s⁻¹ was observed.

On the basis of the FRET between Cy_3 IFN α 2 and AF_{488} ifnar2-H10, the formation and the dynamics of the ternary complex with ifnar1-H10 tethered to the bilayer were studied. Ifnar1-H10 binds IFN α 2 with a very low affinity (~ 5 μ M) and a k_d of ~ 1 s⁻¹.¹⁰ Extensive binding studies have shown that the interactions of IFN α 2 with ifnar1-H10 and ifnar2-H10 are independent of each other (ref

9 and unpublished results). After sequentially tethering AF_{488} ifnar2-H10 and ifnar1-H10 onto the lipid bilayer in a 1:1 molar ratio, Cy_3 IFN α 2 was injected, and the interaction with AF_{488} ifnar2-H10 was monitored by FRET (Figure 2c). Dissociation of the ligand was very slow compared to the interaction with ifnar2-H10 alone, which can be ascribed to the formation of a ternary complex by simultaneous interaction of IFN α 2 with ifnar2-H10 and ifnar1-H10. This ternary complex, however, is in dynamic equilibrium with the binary complexes of IFN α 2 with each of the receptor subunits. To probe the surface kinetics of the interaction with ifnar2-H10, the ternary complex was pulse-chased by tethering a 10-fold excess of nonlabeled ifnar2-H10 over AF_{488} ifnar2-H10 onto the surface within ~ 10 s (Figure 2d). The rise in donor fluorescence intensity indicated AF_{488} ifnar2-H10 dissociation from Cy_3 IFN α 2. No ligand, however, dissociated from the surface under these conditions as confirmed in a control experiment with direct excitation of Cy3 (Figure 2e). Thus, the change in fluorescence was solely due to exchange of OG_{488} ifnar2-H10 in the ternary complex by unlabeled ifnar2-H10, confirming the dynamic nature of the ternary complex. The kinetics monitored by donor fluorescence recovery, therefore, represents the dissociation kinetics of the AF_{488} ifnar2/ Cy_3 IFN α 2 complex in plane of the membrane. Strikingly, significantly slower dissociation was observed under these conditions with a k_d of 0.012 ± 0.003 s⁻¹ (Figure 2f), which was confirmed for different receptor surface concentrations. The reasons for the slower dissociation could be slower diffusion of the proteins in the membrane or the reduced degree of freedom affecting the interaction coordinate. Further studies are required to resolve this issue decisively.

The substantial effect of protein tethering to the membrane on the dissociation kinetics, however, highlights the key importance of mimicking the properties of the membrane for studying ligand–receptor dynamics. Here, we have succeeded to directly determine the dissociation rate constant of an important cytokine–receptor complex in plane of the membrane. The novel, high-affinity bis-NTA lipid provided the key prerequisites of such an endeavor: stable tethering of the proteins to the membrane in an oriented manner, and the possibility to rapidly change the receptor surface concentration. In combination with powerful surface-sensitive techniques for controlling and probing interaction, this provides means for experimentally addressing the role of lateral interaction at the membrane in signaling processes.

Acknowledgment. We thank Robert Tampé for hosting and supporting our group. This work was supported by the DFG (PI 405/1, PI 405/2), and by the BMBF (0312005A).

Supporting Information Available: Description of the synthesis of the bis-NTA lipid, description of the binding assays. This material is available free of charge via the Internet at <http://pubs.acs.org>.

References

- Ullrich, A.; Schlessinger, J. *Cell* **1990**, *61*, 203–212.
- Adam, G.; Delbruck, M. In *Structural Chemistry and Molecular Biology*; Davidson, N., Ed.; W. H. Freeman and Company: New York, 1968; pp 198–215.
- DeLisi, C. Q. *Rev. Biophys.* **1980**, *13*, 201–230.
- Axelrod, D.; Wang, M. D. *Biophys. J.* **1994**, *66*, 588–600.
- Busch, K.; Tampe, R. *J. Biotechnol.* **2001**, *82*, 3–24.
- Dorn, I. T.; Neumaier, K. R.; Tampe, R. *J. Am. Chem. Soc.* **1998**, *120*, 2753–2763.
- Lata, S.; Piehler, J. *Anal. Chem.* **2005**, *77*, 1096–1105.
- Lata, S.; Reichel, A.; Brock, R.; Tampé, R.; Piehler, J. *J. Am. Chem. Soc.* **2005**, *127*, 10205–10215.
- Lamken, P.; Lata, S.; Gavutis, M.; Piehler, J. *J. Mol. Biol.* **2004**, *341*, 303–318.
- Gavutis, M.; Lata, S.; Lamken, P.; Müller, P.; Piehler, J. *Biophys. J.* **2005**, *88*, 4289–4302.

JA054700L